





Studying a correlation between characteristics of rock and their conditions

Arstanbek Abdiev^{1*}, Rakhat Mambetova², Aziz Abdiev¹, Sher Abdiev³

¹Kyrgyz State Mining University, Bishkek, 720001, Kyrgyzstan

²Kyrgyz-Russian Slavic University, Bishkek, 720044, Kyrgyzstan

³State Agency for Architecture, Construction and Housing and Communal Services under the Government of the Kyrgyz Republic, Bishkek, 720001, Kyrgyzstan

*Corresponding author: e-mail abдиев.арстан@mail.ru, tel. +996553799995

Abstract

Purpose is to determine dependences of velocities of elastic waves in isotropic rocks and anisotropic waves with orthotropic and transverse-isotropic symmetry upon pressure and depth to develop evaluation criteria and control rock mass characteristics and conditions in the neighbourhood of mine workings.

Methods. Continuous anisotropic medium is under consideration. Group one of boundary conditions is represented by continuity of stresses, acting normally towards the boundary while transiting from layer 1 to layer 2. Group two of the boundary conditions is as follows: displacements in the process of the boundary transition are measured continuously too. The conditions are necessary to solve a Navier Stokes equation of dynamic balance of absolutely elastic medium. The experiments were carried out with the help of geoaoustic method in terms of the acoustic parameter of compressional velocity.

Findings. It has been determined that compressional velocity values, anisotropy of compressional velocity, and elastic behaviour reflect regularly structural features being pressure-dependent ones. It has been demonstrated that dependence upon the stress state, anisotropy appearance/disappearance emergence takes place or a sign inversion. Qualitative dependences have been obtained to define elastic behaviour (E , μ , G) of anisotropic formation with orthotropic and transverse-isotropic symmetry. The dependences have been obtained through compressional velocity to consider accurately the anisotropy of the rock mass while evaluating its stress state. The research results will help estimate nature of the stress distribution; identify stress concentration zones; and zones of the disturbed rock in the neighbourhood of a mine working. That will be done using acoustic parameter of compressional velocity using a method of geoaoustic control developed by the authors.

Originality. In terms of the new obtained dependences, elastic behaviour of rocks (E , μ , G) as well as acoustic parameters of compressional velocity has been determined scientifically. They are important to design and schedule mining operations.

Practical implications. Being quite accurate to satisfy the demands of practical use, the obtained research results may be applied to identify digital values of elastic behaviour (E , μ , G); to use the method of geoaoustic control of rock mass characteristics and conditions in the neighbourhood of mine workings; and to mine deposits with complex structural and mechanical properties.

Keywords: *isotropic and anisotropic rocks, rock stress, elastic behaviour, acoustic parameter, compressional velocity, geoaoustic control*

1. Introduction

Disturbance of the initial stress by means of mining operations results in the significant stress concentration; within certain areas of the rock mass in the neighbourhood of outcrops it may factor into initiation of extremely complicated geomechanical processes exercising a dominant influence on the safety of mining and its efficiency [1]-[4]. Deformations after outcrop origination continue in time; thus, failure is possible in terms of stresses being quite less than the rock strength [5], [6]. Solving a number of important practical problems depends upon regularities of the development of geomechanical processes. Analytical methods to evaluate outcrop stability in the

neighbourhood of mine workings cannot explain a field of stress distribution in rock mass [7]-[10].

That is why it is necessary to use a method of geoaoustic control of rock mass characteristics and conditions in the neighbourhood of mine workings as a simple and operational experimental technique making it possible to analyze rocks under full-scale conditions with a possibility of the unlimited measurement repetition within the analyzed point with no rock mass disturbance [11], [12]. Acoustic parameter of a compressional velocity, determined through regularities of elastic behaviour and compressional velocity of rocks, are the basic informative parameters of geoaoustic control. The matter is that naturally anisotropy of rock properties causes changes in the

principles of stress and deformation distribution while effecting the nature of acoustic characteristic distribution within them.

Numerous scientific sources concern the problem of elastic behaviour of anisotropic rocks through the velocities of elastic waves [13]-[15]. For the cases of thin-layer medium $\lambda \gg h_1 h_2$, papers [16]-[20] determine wave velocities through average values of elasticity coefficients $K_{||}$ and K_{\perp} corresponding static purely compressional and lateral deformations along the bedding and transversely to it. However, the cases did not involve calculation of velocity changes depending upon the wave propagation angle. Papers [21]-[25] considered propagation of elastic waves within the diametric-isotropic and transverse-isotropic media. As a result, dependences of elastic wave velocities within two orthogonally related directions upon a seismic beam exit were obtained. Moreover, elastic wave velocities have been calculated taking into consideration the specified elasticity constants G_{ik} , and meaningful coefficient of stress-deformation linear connection [26]-[29]. Representing orthotropic medium as imposition of two lateral-isotropic media, group three of papers has obtained values of elastic wave velocities for orthotropic medium relying upon values of elasticity constants G_{ik} .

Papers [30]-[32] focus on kinematic characteristics of elastic wave propagation within the anisotropic media; and calculation of phase wave surfaces and wave ones. Such studies help determine approximately the velocity values in terms of some tendency as for the medium homogeneity and isotropism [33]-[36]. Hence, the problem of wave propagation within the layered media is not clearly understood which can be explained by the complexity of its theoretical description.

2. The research methods

Generally, anisotropic medium is represented as the organized alternate two layers with varying different h_1 and h_2 thicknesses; different elastic constants E_1 and E_2 ; different wave propagation velocities; and different ρ_1 and ρ_2 densities. Since the medium is considered as a continuous one, elastic disturbances transfer from one its part to another. Hence, certain connection is available between the stresses and deformations of particles located on the opposite sides of the boundary. In terms of isotropic body and anisotropic one, the connection between stress components and deformation components is described either through the generalized Hooke's law or through the deformation components. They are mutually defined.

Group one of the conditions within a boundary is represented by stress continuity conditions acting normally towards the boundary while transiting from layer 1 to layer 2. Group two of boundary conditions is as follows: shifts in the process of the boundary crossing are measured continuously too. The conditions are necessary to solve an equation of dynamic balance of absolutely elastic medium. In terms of a vector form, it is the Navier Stokes equation:

$$\rho = \frac{d^2 \bar{U}}{dt^2} = (\lambda + \mu) \cdot \text{grad} \cdot \text{div} \bar{U} + \mu \nabla^2 \bar{U}, \quad (1)$$

where:

λ and μ – Lamé constants determining elastic behaviour of a medium.

If displacement filed U in elastic medium is connected with scalar potential φ and vector potential $\vec{\psi}$:

$$U = \text{grad} \varphi + \text{rot} \vec{\psi}, \quad (2)$$

then equation (2) falls into the two independent wave equations:

$$\frac{d^2}{dt^2} \cdot \text{rot} \bar{U} = \frac{\mu^2}{\rho} \cdot \nabla^2 \text{rot} \bar{U}; \quad (3)$$

$$\frac{d^2}{dt^2} \cdot \text{div} \bar{U} = \frac{(\lambda + 2\mu)}{\rho} \cdot \nabla^2 \text{div} \bar{U}. \quad (4)$$

Independent equations (3) and (4) are indicative of the availability of two disturbance types within the limitless elastic medium. The disturbances are propagated with two physically different velocities – compressional velocity and lateral velocity.

In the context of anisotropic media, λ and μ values depend upon the space coordinates. Since changes in velocities exceed significantly changes in density, then medium density is averaged in terms of its volume being specified as a constant one. In general, velocities of elastic wave propagation within the anisotropic media are identified by means of an equation involving 21 elastic constants G_{ik} , density ρ , and direction of oscillation propagation \vec{n} . The equation of elastic medium motion may be expressed in the following compact form:

$$\rho V^2 P_{ki} = C_{ik} P_{ok} n_j n_e, \quad (5)$$

where:

$P(\bar{U}, V, W)$ – components of a displacement vector.

Displacement components in a plane wave may be represented as follows:

$$P = P_o e^{i(\omega t - kr)},$$

where:

k – is a wave vector.

Normal incidence to a plane boundary of media separation of a plane compressional wave P results in the origination of one quasi-compressional wave and two quasi-transverse waves within the medium: SV – when the transverse wave is polarized in the incidence plane; and SH – when the transverse wave is polarized perpendicularly to the incidence plane. Increase in the incidence factors into origination of the converted waves.

Equation (5) involves three positive roots corresponding to three velocities of elastic wave propagation within the elastic body. Generally, their values depend upon elastic constant media as well as upon a direction of the wave propagation relative to elastic symmetry axes determined by l , m and n values (they are constant for any directions in terms of isotropic medium).

In general, three independent waves with mutually perpendicular displacements are propagated in any direction irrespective of a degree of the medium anisotropy. However, components of displacement vectors not always coincide with a direction of wave propagation and normally to the wave front. Put it differently, in the general case elastic waves are neither purely compressional waves nor purely transversal ones. Nevertheless, there are specific directions in crystals along which a normal to a wave front coincides with a displacement vector of one of the three waves being purely

compressional. Considering that their displacement vectors are mutually perpendicular, displacement vectors of two other waves are within the wave front plane. Thus, separation of purely compressional and purely transversal is only possible in media having certain symmetry of elastic properties. It is common knowledge that within anisotropic medium, seismic waves are not orthogonal to a wave front and elastic wave velocity depends upon \bar{n} direction. That is why ultrasonic measurements consider velocities towards a normal to the front. The research uses values of velocities of compressional and transversal waves propagating towards reference axes. Subsequently, the case in hand will be the waves only.

Since rocks are characterized by anisotropy as well as elastic and acoustic properties, theoretical evidence are required to make it possible to determine elastic characteristics of anisotropic rocks using geoaoustic methods.

The research does not apply values of linear connection G_{ik} coefficients being extremely important for crystallography but elastic characteristics of media having a direct physical meaning: elasticity modulus E , shear modulus G , and Poisson's ratio μ . To achieve the goal, below a problem to determine elastic characteristics of anisotropic rocks in terms of elastic wave velocities is considered.

3. Results and discussion

3.1. Analysis of elastic properties of anisotropic rock mass

3.1.1. Rock with orthotropic symmetry

Generally, in terms of elastic symmetry, anisotropic rocks may be classified as orthotropic media with nine independent elastic constants. In terms of the medium, each separated elementary volume demonstrates three mutually perpendicular reference axes. Symmetrically, they are similar to crystals of a rhombic system. If availability of symmetry of properties is assumed then the number of elastic constants, determining conditions of orthotropic body, reduces from 21 down to 9: C_{11} , C_{12} , C_{22} , C_{13} , C_{23} , C_{33} , C_{44} , C_{55} and C_{66} ; other constants will be equal to zero.

As a rule, engineering tests use constants having a direct physical meaning rather than such values as a_{ik} and C_{ik} . If so, the generalized Hooke's law for orthotropic media through physical constants is expressed as follows:

$$\begin{aligned}\varepsilon_x &= \frac{1}{E_x} \cdot \sigma_x - \frac{\mu_{xy}}{E_y} \cdot \sigma_y - \frac{\mu_{xz}}{E_z} \cdot \sigma_z; \\ \varepsilon_y &= -\frac{\mu_{yx}}{E_x} \cdot \sigma_x + \frac{1}{E_y} \cdot \sigma_y - \frac{\mu_{yz}}{E_z} \cdot \sigma_z; \\ \varepsilon_z &= -\frac{\mu_{zx}}{E_x} \cdot \sigma_x - \frac{\mu_{zy}}{E_y} \cdot \sigma_y + \frac{1}{E_z} \cdot \sigma_z,\end{aligned}\quad (6)$$

hence:

$$\begin{aligned}E_y \mu_{yx} &= E_x \mu_{xy}; \\ E_z \mu_{zy} &= E_y \mu_{yz}; \\ E_x \mu_{zx} &= E_z \mu_{xz},\end{aligned}\quad (7)$$

Elastic properties of anisotropic body with three axes of elastic symmetry are characterized by following types of elastic constants: three elasticity moduli – E_x , E_y , and E_z ; three shear moduli – G_{yz} , G_{zx} , and G_{xy} ; and three Poisson's

ratios – μ_{yz} , μ_{zx} , and μ_{xy} (three other constants, resulting from rearrangement of indices, are not independent).

To evaluate anisotropy effect on elastic properties of the media, it is necessary to study them from the viewpoint of three lines at least. Determination of complete set, involving nine elastic constants, is quite sufficient to evaluate the effect of elastic property anisotropy on the stress distribution within the orthotropic medium.

Through physical constants, values of elastic constants for orthotropic medium are as follows:

$$\begin{aligned}C_{11} &= \frac{1 - \mu_{yz} \mu_{zy}}{\bar{\Delta}} E_x; \\ C_{22} &= \frac{1 - \mu_{xz} \mu_{zx}}{\bar{\Delta}} E_y; \\ C_{33} &= \frac{1 - \mu_{xy} \mu_{yx}}{\bar{\Delta}} E_z; \\ C_{12} &= \frac{\mu_{yx} + \mu_{zx} \mu_{yz}}{\bar{\Delta}} E_y; \\ C_{13} &= \frac{\mu_{zx} + \mu_{zy} \mu_{yx}}{\bar{\Delta}} E_z; \\ C_{23} &= \frac{\mu_{zy} + \mu_{zx} \mu_{xy}}{\bar{\Delta}} E_y; \\ C_{44} &= C_{23}; \\ C_{55} &= C_{31}; \\ C_{66} &= C_{12},\end{aligned}\quad (8)$$

where:

$\bar{\Delta}$ symbolizes a determinant:

$$\bar{\Delta} = \begin{vmatrix} 1 & \mu_{xy} & \mu_{xz} \\ -\mu_{yx} & 1 & -\mu_{yz} \\ -\mu_{zx} & \mu_{zy} & 1 \end{vmatrix}, \quad (9)$$

hence,

$$\bar{\Delta} = 1 - \mu_{xy} \mu_{yx} - \mu_{yz} \mu_{zy} - \mu_{zx} \mu_{xz} - 2\mu_{xy} \mu_{yz} \mu_{zx}. \quad (10)$$

Determinant equation for anisotropic body with average ρ density, within which elastic wave propagates, is:

$$\begin{vmatrix} C_{11}l^2 + C_{66}m^2 + C_{55}n^2 - \rho V^2 & (C_{12} + C_{66})lm(C_{13} + C_{55})nl \\ (C_{12} + C_{55})lmC_{66}l^2 + C_{22}m^2 + C_{44}n^2 - \rho V^2 & (C_{23} + C_{44})mn \\ (C_{13} + C_{55})nl(C_{23} + C_{44})mnC_{55}l^2 + C_{44}m^2 + C_{33}n^2 - \rho V^2 \end{vmatrix} = 0. \quad (11)$$

Relying upon (11), obtain three equation system with corresponding set of elastic constants:

$$\begin{aligned} & [C_{11}l^2 + C_{66}m^2 + C_{55}n^2 - \rho V^2] \cdot P_{01} + \\ & + [(C_{12} + C_{66}) \cdot lm] \cdot P_{02} + [(C_{13} + C_{55}) \cdot nl] \cdot P_{03} = 0; \end{aligned}\quad (12)$$

$$\begin{aligned} & [(C_{12} + C_{66}) \cdot lm] \cdot P_{01} + [C_{66}l^2 + C_{22}m^2 + C_{44}n^2 - \rho V^2] \times \\ & \times P_{02} + [(C_{23} + C_{44}) \cdot mn] \cdot P_{03} = 0; \end{aligned}\quad (13)$$

$$\begin{aligned} & [(C_{13} + C_{55}) \cdot nl] \cdot P_{01} + [(C_{23} + C_{44}) \cdot mn] \cdot P_{02} + \\ & + [C_{55}l^2 + C_{44}n^2 + C_{33}n^2 - \rho V^2] \cdot P_{03} = 0. \end{aligned}\quad (14)$$

Consider geometric configuration of a rhombic system with a system of orthotropic symmetry, corresponding to it (Fig. 1a). As it has been mentioned, a normal towards a wave front coincidence with a displacement vector is a condition of purely compression wave propagation. Then, two other waves, being perpendicular to it, will be transversal ones. Let a plane axial wave propagates along x axis in terms of the system, superimposed with the coordinate axes x , y and z . $l = 1$, $m = 0$ and $n = 0$ condition corresponds to that. Thus, using equation system (12)-(14) we find:

$$\begin{aligned} (C_{11} - \rho V^2) \cdot P_{01} &= 0; \\ (C_{66} - \rho V^2) \cdot P_{02} &= 0; \\ (C_{55} - \rho V^2) \cdot P_{03} &= 0. \end{aligned} \quad (15)$$

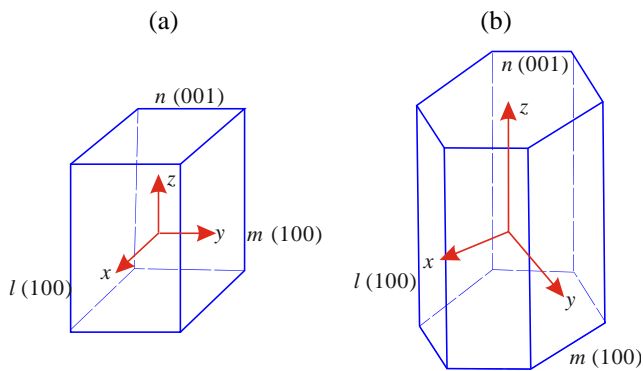


Figure 1. Geometrical configuration of rhombic symmetry (a) and hexagonal symmetry (b)

It follows that propagation velocity of a compression wave along axis x is determined using the ratio:

$$\rho V_{P_x}^2 = C_{11}, \quad (16)$$

in terms of a transversal wave, propagating in the same line but polarized within xy plane and being perpendicular to orthogonal axis, we obtain:

$$\rho V_{S_{xy}}^2 = C_{66}. \quad (17)$$

In terms of a transversal wave towards x axis but polarized within xz plane we have:

$$\rho V_{S_{xz}}^2 = C_{55}. \quad (18)$$

If a wave propagates along y axis, i.e. $l = 0$, $m = 1$ and $n = 0$, then the equation system (12)-(14) will help to write the following:

$$\begin{aligned} (C_{66} - \rho V^2) \cdot P_{01} &= 0; \\ (C_{22} - \rho V^2) \cdot P_{02} &= 0; \\ (C_{44} - \rho V^2) \cdot P_{03} &= 0. \end{aligned} \quad (19)$$

Thus, a velocity of compressional wave propagation along y axis, and velocities of transversal waves, propagating along y axis but polarized in yz and yx plane, are determined using the ratios:

$$\rho V_{P_y}^2 = C_{22}; \quad (20)$$

$$\rho V_{S_{yz}}^2 = C_{44}; \quad (21)$$

$$\rho V_{S_{yx}}^2 = C_{66}. \quad (22)$$

$l = 0$, $m = 0$ and $n = 1$ is fulfilled for a wave propagating along z axis. Then equation system (12)-(14) will be:

$$\begin{aligned} (C_{55} - \rho V^2) \cdot P_{01} &= 0; \\ (C_{44} - \rho V^2) \cdot P_{02} &= 0; \\ (C_{33} - \rho V^2) \cdot P_{03} &= 0. \end{aligned} \quad (23)$$

Same as previous, propagation velocities of compression wave and transversal wave towards orthogonal axis, polarized within a zy , zx plane, are identified using the ratio:

$$\rho V_{P_z}^2 = C_{33}; \quad (24)$$

$$\rho V_{S_{zx}}^2 = C_{55}; \quad (25)$$

$$\rho V_{S_{zy}}^2 = C_{44}. \quad (26)$$

Consequently, (16)-(18), (20)-(22), and (24)-(26) ratios have been obtained for the orthogonal symmetry rocks having three axes of elastic symmetry. The ratios interconnect the velocities of elastic wave propagation along the certain axes with elastic medium constants. As the formulas explain, three waves with orthogonal displacements propagate along each axis of elastic symmetry: one compressional wave (i.e. quasi-compressional wave) and two transversal waves (i.e. quasi-transversal ones). Since it is known that rays are not perpendicular to a wave front in anisotropic media, it is necessary to consider two velocities: a velocity in the ray line and a velocity in the normal line towards the wave front (subsequently, the velocities will be the issue). Inserting corresponding values of elastic constants from (3)-(4) equations we obtain the following:

– along axis x direction:

$$\rho V_{P_x}^2 = \frac{1 - \mu_{yz}\mu_{zy}}{\Delta} \cdot E_x; \quad (27)$$

– along axis y direction:

$$\rho V_{P_y}^2 = \frac{1 - \mu_{xz}\mu_{zx}}{\Delta} \cdot E_y; \quad (28)$$

– along axis z direction:

$$\rho V_{P_z}^2 = \frac{1 - \mu_{xy}\mu_{yx}}{\Delta} \cdot E_z; \quad (29)$$

$$\rho V_{S_{zx}}^2 = G_{zx}.$$

Substitute for $\bar{\Delta}$ its value from formula (9). Therefore, we obtain the dependence for limitless orthotropic medium with three orthogonal reference axes:

$$\begin{aligned} E_x &= \frac{V_{P_x}^2 \cdot \rho (1 - \mu_{xy}\mu_{yx} - \mu_{yz}\mu_{zy} - \mu_{zx}\mu_{xz} - 2\mu_{xy}\mu_{yz}\mu_{zx})}{g(1 - \mu_{yz}\mu_{zy})}; \\ E_y &= \frac{V_{P_y}^2 \cdot \rho (1 - \mu_{xy}\mu_{yx} - \mu_{yz}\mu_{zy} - \mu_{zx}\mu_{xz} - 2\mu_{xy}\mu_{yz}\mu_{zx})}{g(1 - \mu_{zx}\mu_{xz})}; \\ E_z &= \frac{V_{P_z}^2 \cdot \rho (1 - \mu_{xy}\mu_{yx} - \mu_{yz}\mu_{zy} - \mu_{zx}\mu_{xz} - 2\mu_{xy}\mu_{yz}\mu_{zx})}{g(1 - \mu_{xy}\mu_{yx})}. \end{aligned} \quad (30)$$

Shear moduli along the key directions are:

$$\begin{aligned} G_{xy} &= \frac{V_{Sxy}^2 \cdot \rho}{g}; \\ G_{yz} &= \frac{V_{Syz}^2 \cdot \rho}{g}; \\ G_{zx} &= \frac{V_{Szx}^2 \cdot \rho}{g}, \end{aligned} \quad (31)$$

where:

E_x , E_y and E_z – elasticity moduli in terms of the key directions;

G_{xy} , G_{yz} and G_{zx} – shear moduli within the key shear planes;

μ_{xy} , μ_{yz} , μ_{zx} , μ_{yx} , μ_{zy} and μ_{xz} – Poisson’s ratios for the corresponding planes of symmetry.

Their values may be determined in terms of compressional and transversal waves measured in corresponding lines; ρ is rock density; and g is gravity acceleration. Complete characteristic of orthotropic rock mass should also involve Poisson’s ratio values according in terms of different axes of elastic symmetry.

To do that, it is necessary to consider shear wave propagation at some α angle towards the key directions. Let the key directions coincide with x , y and z axes; shear wave propagates in the line of x being polarized within $x'y'$ plane.

Then, Hook’s law for angular deformations will be:

$$\varepsilon_{y'x'} = \frac{1}{G_{y'x'}} \tau_{x'y'}, \quad (32)$$

where:

$$\frac{1}{G_{y'x'}} = \left(\frac{1 - \mu_{xy}}{E_x} + \frac{1 - \mu_{xy}}{E_y} - \frac{1}{E_{xy}} \right) \cdot \sin 2\alpha + \frac{1}{G_{xy}}. \quad (33)$$

In terms of $\alpha = 45^\circ$:

$$G_{xy}^{45^0} = \frac{E_x}{1 + 2\mu_{xy} + \frac{E_x}{E_y}}. \quad (34)$$

Hence:

$$\mu_{xy} = \frac{E_y \cdot \left(E_x + G_{xy}^{45^0} \right) - 2E_x G_{xy}^{45^0}}{2G_{xy} E_x}. \quad (35)$$

Similar operations help obtain expressions for Poisson’s ratios in other two directions (i.e. μ_{zx} , and μ_{yz}).

In practical terms, μ_{zx} , μ_{yz} , and μ_{xy} Poisson’s ratios can be determined with the help of velocities of compressional and transversal waves measured along the key anisotropic lines, i.e.:

$$\begin{aligned} \mu_{xy} &= \frac{V_{Px}^2 - 2V_{Sxy}^2}{2(V_{Px}^2 - 2V_{Sxy}^2)}; \\ \mu_{yz} &= \frac{V_{Py}^2 - 2V_{Syz}^2}{2(V_{Py}^2 - 2V_{Syz}^2)}; \\ \mu_{zx} &= \frac{V_{Pz}^2 - 2V_{Szx}^2}{2(V_{Pz}^2 - 2V_{Szx}^2)}. \end{aligned} \quad (36)$$

Other three Poisson’s ratios (i.e., μ_{xy} , μ_{yz} , and μ_{zx}) are independent ratios. Hence, availability of (30), (31), and (36) dependences makes it possible to define each dynamic elastic characteristic of anisotropic rock with orthotropic elastic symmetry. To do that, it is required to identify velocity values of compressional waves and transversal waves along the key lines of elastic symmetry axes as well as velocity values of transversal waves at 45° angle to the key directions.

3.1.2. Rock with transverse-isotropic symmetry

Anisotropic (i.e. sedimentary) rocks are of a transverse-isotropic type with elastic symmetry and five elastic constants. Such a symmetry type is characteristic for the stratified rocks. All the lines within a plane of the laminated layers are equal to each other; hence, the stratification plane will be isotropic plane and an axis, being perpendicular to it, will be a symmetry axis of an infinite order.

In this context, the generalized Hook’s law, expressed through physical constants, will be of the form:

$$\begin{aligned} \varepsilon_x &= \frac{1}{E_x} \sigma_x - \frac{\mu_{xy}}{E_y} \sigma_y - \frac{\mu_{zx}}{E_z} \sigma_z; \\ \varepsilon_y &= -\frac{\mu_{yx}}{E_x} \sigma_x + \frac{1}{E_x} \sigma_y - \frac{\mu_{zy}}{E_z} \sigma_z; \\ \varepsilon_z &= -\frac{\mu_{zx}}{E_x} \sigma_x - \frac{\mu_{zy}}{E_x} \sigma_y + \frac{1}{E_z} \sigma_z; \\ \varepsilon_{yz} &= \frac{1}{G_{yz}} \tau_{yz}; \\ \varepsilon_{zx} &= \frac{1}{G_{zx}} \tau_{zx}; \\ \varepsilon_{xy} &= \frac{2(1 - \mu_{xy})}{G_{xy}} \tau_{xy}. \end{aligned} \quad (37)$$

If axis z is assumed as an axis of an infinite order and xy axis is assumed as an isotropic plane then substitution of all y and x indices from (7) will result in:

$$\begin{aligned} \frac{1}{E_x} &= \frac{1}{E_y}; \\ \frac{\mu_{zx}}{E_x} &= \frac{\mu_{xz}}{E_z}; \\ \frac{\mu_{zx}}{E_x} &= \frac{\mu_{zy}}{E_y} = \frac{\mu_{xz}}{E_z} = \frac{\mu_{yz}}{E_z}. \end{aligned} \quad (38)$$

In this context, the number of elastic constants, characterizing condition of the medium is equal to 5: C_{11} , C_{12} , C_{22} , C_{13} , C_{33} , C_{44} , and $C_{66} = \frac{C_{11} - C_{12}}{2}$. Other elastic constants are equal to zero.

In terms of symmetry, such media are similar to crystals of a hexagonal system.

Determinant equation for a transverse-isotropic medium with ρ density within which elastic waves with velocities propagate will be expressed as follows:

$$\left\{ \begin{array}{l} C_{11}l^2 + \frac{1}{2}(C_{11} - C_{12})m^2 + C_{44}n^2 - \rho V^2 \\ \frac{1}{2}(C_{11} + C_{12})lm(C_{11} + C_{12})nl \\ \frac{1}{2}(C_{11} + C_{12})lm \frac{1}{2}(C_{11} - C_{12})l^2 + C_{11}m^2 + C_{44}n^2 - \rho V^2 \\ (C_{13} + C_{44})mn \\ (C_{13} + C_{44})nl(C_{13} + C_{44})mnC_{44}(l^2 + m^2) + C_{33}n^2 - \rho V^2 \end{array} \right\} = 0. \quad (39)$$

Similarly to a case of orthotropic body, it is possible to obtain following equations using an equation of motion in elastic medium:

$$\begin{aligned} & \left[C_{11}l^2 + \frac{1}{2}(C_{11} - C_{12})m^2 + C_{44}n^2 - \rho V^2 \right] \cdot P_{01} + \\ & + \left[\frac{1}{2}(C_{11} - C_{12})lm \right] \cdot P_{02} + [(C_{13} - C_{44})nl] \cdot P_{03} = 0; \\ & \left[\frac{1}{2}(C_{11} + C_{12})lm \right] \cdot P_{01} + \\ & + \left[\frac{1}{2}(C_{11} + C_{12})l^2 + C_{11}m^2 + C_{44}n^2 - \rho V^2 \right] \times \\ & \times P_{02} + [(C_{13} + C_{44})mn] \cdot P_{03} = 0; \\ & [(C_{13} + C_{44})nl] \cdot P_{01} + [(C_{13} + C_{44})mn] \cdot P_{02} + \\ & + [C_{44}(l^2 + m^2) + C_{33}n^2 - \rho V^2] \cdot P_{03} = 0. \end{aligned}$$

If a wave propagates along hexagonal axis x (Fig. 1b) then that corresponds to $l = 1$, $m = 0$ and $n = 0$ condition resulting in the equation system (39) simplification:

$$\begin{aligned} & [C_{11} - \rho V^2] \cdot P_{01} = 0; \\ & \left[\frac{1}{2}(C_{11} + C_{12}) - \rho V^2 \right] \cdot P_{02} = 0; \\ & [C_{44} - \rho V^2] \cdot P_{03} = 0. \end{aligned} \quad (40)$$

Hence, in terms of a compressional wave, propagating along x axis, we have:

$$\rho V^2 P_x = C_{11}, \quad (41)$$

in terms of a transversal wave, propagating towards x axis, polarized in xz plane, we have:

$$\rho V^2 S_{xz} = C_{44}. \quad (42)$$

In terms of a wave, polarized within xy plane but propagating along x axis, we have:

$$\rho V^2 P_x = \frac{1}{2}(C_{11} - C_{12}) = C_{66}. \quad (43)$$

If a wave propagates along hexagonal axis z , then $l = 0$, $m = 0$ and $n = 1$. Thus, we obtain the equations:

$$\begin{aligned} & [C_{44} - \rho V^2] \cdot P_{01} = 0; \\ & [C_{33} - \rho V^2] \cdot P_{03} = 0. \end{aligned} \quad (44)$$

Hence, for a compressional wave, propagating towards z axis, we have:

$$\rho V^2 P_z = C_{33}. \quad (45)$$

In terms of a transversal wave, propagating along z axis but polarized within xz plane, we have:

$$\rho V^2 S_{zx} = C_{44}. \quad (46)$$

Substituting values of elastic constants into (42), (43), (44), (45), and (46) for elastic characteristics of transverse-isotropic body, we have:

$$E_x = \frac{V^2 P_x \cdot \rho}{g} - \frac{\bar{\Delta}}{1 - \mu_{yz}\mu_{zy}}; \quad (47)$$

$$E_z = \frac{V^2 P_z \cdot \rho}{g} - \frac{\bar{\Delta}}{1 - \mu_{xy}\mu_{yz}}.$$

$$G_{xy} = \frac{V_{sxy}^2 \cdot \rho}{g}; \quad (48)$$

$$G_{zx} = \frac{V_{szx}^2 \cdot \rho}{g}.$$

Transverse-isotropic body is characterized by five elastic constants E_1 , E_2 , G_2 , μ_1 , μ_2 . In the context of coordinate system with z axis, being perpendicular to a plane of isotropy xy , specifying:

$$\begin{aligned} E_x &= E_y = E_1; \\ E_z &= E_2; \\ G_{xy} &= G_1; \\ G_{zx} &= G_2; \\ \mu_{xy} &= \mu_{yx} = 1; \\ \mu_{yz} &= \mu_{zy} = \mu_2, \end{aligned} \quad (49)$$

and taking into consideration (46) and (47) for anisotropic rocks with transverse-isotropic symmetry we obtain:

$$E_1 = \frac{V^2 P_x \cdot \rho}{g} \cdot \frac{(1 - \mu_1) \cdot (1 - \mu_1 - 2\mu_2^2)}{1 - \mu_2^2}; \quad (50)$$

$$E_2 = \frac{V^2 P_z \cdot \rho}{g} \cdot \frac{(1 - \mu_1 - 2\mu_2^2)}{(1 - \mu_1)}; \quad (51)$$

$$G_2 = \frac{V^2 S_{xz} \cdot \rho}{g}. \quad (52)$$

where:

E_1 – elasticity modulus for lines within the plane of isotropy;
 E_2 – elasticity modulus for lines being perpendicular to the plane of isotropy;

G_2 – shear modulus for planes being perpendicular to the plane of isotropy;

μ – Poisson's ratio characterizing deformation within the plane of isotropy subject to the same plane force;

μ_1 – Poisson's ratio characterizing deformation within a plane of isotropy under tension in a perpendicular line;

μ_2 – Poisson's ratio characterizing deformation within a plane being perpendicular to the plane of isotropy.

Such Poisson's ratios as μ , $\mu_1 = \mu_{zx}$, and $\mu_2 = \mu_{xz}$ can be obtained using velocity values of compressional and shear waves in terms of corresponding directions.

(36) and (50)-(52) dependences help determine values of elasticity moduli as well as values of shear of anisotropic rocks with transverse-isotropic symmetry using elastic wave velocities identified in the two key directions: along stratification, and transverse to it. For this purpose, it is necessary to know velocities of elastic waves (V_P , V_S) along the key axes of elastic symmetry.

Consequently, the identified quantitative dependences make it possible to calculate elastic characteristics of anisotropic rocks on the velocities of compressional and transversal waves measured along the key axes of elastic symmetry as well as velocities of transversal waves at 45° angle to the lines.

To verify the derived quantitative dependences, it is necessary to define analytical scheme of anisotropy the rock belongs to: to media with orthotropic or transverse-isotropic elastic symmetry. That is connected with determination of values, and the key anisotropic lines of the rocks under analysis.

3.2. Dependence of elastic wave velocities within isotropic and anisotropic rocks upon pressure

Along with pressure increase, all rocks demonstrate increase in elastic wave velocities. The velocity increase starts as soon as pressure is applied coming to its end depending upon rock types when load achieves 30-70% of a failure pressure. In terms of similar load intensity, increase in a compressional wave velocity exceeds increase in a transversal wave velocity. That is why study of stress rock mass using geoaoustic method as an informative parameter and the most important technological parameter should involve a value of a compressional wave being the handiest parameter. Since the basic velocity change is observed in the line of a load axis value of the compressional wave velocity increment helps evaluate nature of stress distribution within the rock mass.

Laboratory tests $V_{P,S} = f(\sigma_{comp})$ are widely used while analyzing stress state of rock mass. However, the tests are not sufficient; thus, a method of multiparameter control of characteristics and stress-strain state of rocks is proposed to be used at a research stage.

In the context of homogenous isotropic rocks, compressional wave velocity increases almost linearly at a stage of elastic deformation along with pressure increase.

Influence curve $V = f(p)$ approaches its saturation level while completing a densification process. Compression of different defects terminates; velocity increase slows down. Subsequent load increment results in rock discontinuity and in the velocity decrease. Further progress of the process factors into rock disintegration.

It should be noted that informativeness of functional dependences varies for different loading cases. In terms of linear pressure and uniform pressure, changes in velocities of compressional waves are minor being within the accuracy of laboratory tests.

As for the anisotropic rocks, nature of $V = f(p)$ curve depends upon the wave propagation direction relative to the applied load line. Changes in velocities of compressional waves at loads, oriented diversely relative to stratification take place differently. Stratification curve $V_{P1} = f(p)$ has greater values to compare with a curve of transverse stratification $V_{P\perp} = f(p)$.

Analysis of experimental data, concerning dependence of velocities of elastic waves upon pressure, shows that velocity increment value helps evaluate nature of stress distribution within rock mass. Rocks with isotropic symmetry and aniso-

tropic symmetry have been selected to observe the regularities in terms of the specific rocks and use them for full-scale experiments. Nature of $V_P = f(\sigma)$ dependence has been identified by means of uniaxial compression tests with simultaneous scanning (Fig. 2).

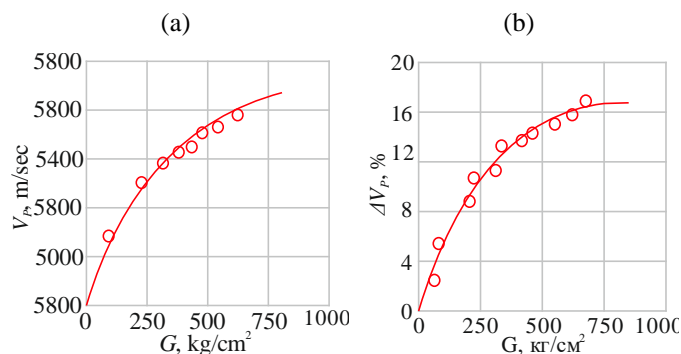


Figure 2. Dependence of a compressional wave velocity (a) and its increments (b) upon pressure in terms of the silicified jasperoids

Strain-gauge station and hydraulic press have been applied to determine statistically deformation characteristics. Oscillograph with loop galvanometers kept the records. The scheme made it possible to obtain broad deformation pattern before disintegration. Electrical facilities used to operate with the sensors. The facilities are quite accurate to record automatically minor resistance changes.

If deformation characteristics of anisotropic media with three axes of elastic symmetry then resistance strain sensors are located differently relative to elastic symmetry axes. A scheme of the strain sensor attachment to the oriented samples helps determine E and μ values along the key symmetry lines. A force to a sample, located between press plates, is applied along axis being parallel to a larger side of a parallelepiped. The loading is performed step by step with a short-period interval to take a reading. Purpose-made sensor matrices with 200 Hz resonance frequency are placed between a press plate and a sample. Ultrasounds device records simultaneously time of flight of acoustic wave pulse for the loading step.

As for the isotropic rocks, the main velocity increment is observed in the line of compressive load action. Total velocity increment along here achieves 30%; in terms of certain samples the increase is up to 35% if the load intensifies from zero to a critical one. More than fourfold velocity increment exceeds natural variability natural of characteristics of the rocks under analysis (Fig. 2b).

Dependence of propagation velocity of elastic waves in anisotropic rocks upon pressure was analyzed with the help of cylindrical and prismatic rock samples representing a wide range of rocks with varying anisotropy degrees.

The tests were carried out in the lines of elastic symmetry axes. Graphs of velocities of elastic waves were constructed separately for each line; pressure changes along the line were also involved. Totality of the dependences makes it possible to control both qualitative and quantitative changes in the velocities of elastic waves as well as anisotropy coefficients of the elastic waves depending upon load application line relative to anisotropy axes.

According to the specified procedure, samples of the laminated limestones, jasperoids, and shales were tested in two orthogonal directions: along stratification (i.e. along fissility)

and transversely to stratification (i.e. transversely to fissility. Samples of micaceous-quartz shales were tested in three directions: to the dip; along the strike; and transversely to stratification of layers.

Tests of the samples have demonstrated that in terms of loading being parallel to stratification, a curve of velocity changes with $V_{P1} = f(p)$ pressure is located quite higher to compare with $V_{P1} = f(p)$ curve when transversely to fissility loading is performed (Fig. 3).

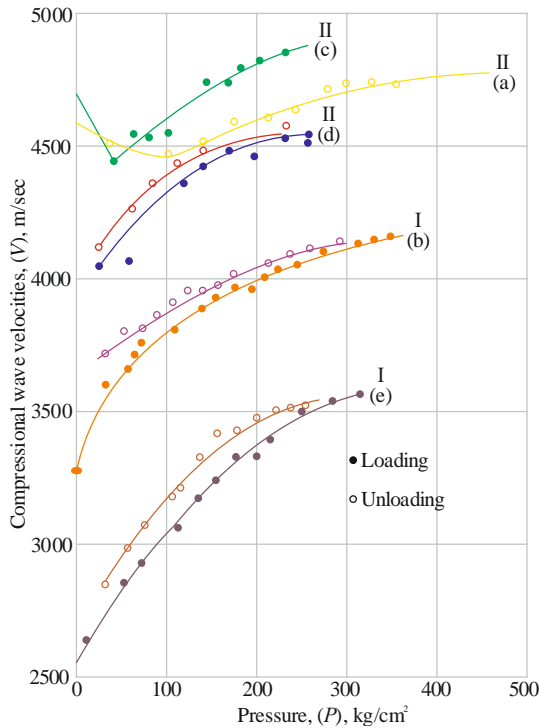


Figure 3. Changes in a velocity of a compressional wave with pressure for the laminated limestones I: (a) loading along fissility; (b) transverse to fissility loading. Changes in a velocity of a compressional wave with pressure for micaceous-quartz shales II: (c) loading to the dip; d is loading along the strike; (d) transverse to stratification loading

Loading process shows the increased velocity of compressional waves with pressure increase; its increment is not uniform throughout the loading cycle: first, velocity with pressure increase intensifies; then, velocity increase starts slowing down being behind pressure increment. In terms of loads, being 50% of critical ones, velocity increment following pressure increase $V_{P1} = f(p)$ taking place transversely to stratification is ~30% for the laminated limestones; 35% for micaceous-quartz shales; and ~20% for jasperoids. In terms of loading along stratification $V_{P1} = f(p)$ it is ~7% for the laminated limestones; and ~10% for micaceous-quartz shales.

Relative increments of compressional waves with pressure were determined using the formula:

$$\frac{\Delta V}{V} = \frac{V_P - V_0}{V_0} \cdot 100 \%, \quad (53)$$

where:

V_P – a compressional wave velocity in terms of pressure P ;
 V_0 – a compressional wave velocity within a sample under the nonloaded condition.

Propagation of elastic waves within a solid body happens the faster the tighter the medium is, and the less disconnections between particles are. Generally, velocity value of a compressional wave, determined along layers for the non-loaded samples is higher than a wave velocity determined transversely to layers.

In terms of tests, carried out transversely to fissility, $V_P = f(p)$ a curve of micaceous-quartz shales for load cycle is situated lower than a curve for unload cycle (Fig. 3); i.e., hysteresis loops are available. Difference in velocity values in the process of loading/unloading is not more than 3% corresponding to the limit of measurement accuracy.

When samples are loaded along fissility within initial load zone, compressional wave velocity decreases down to a definite load (~100 kg/cm²). Then, the velocity increase starts along with pressure increase. In this context, the pressure is less to compare with a case when loading takes place transversely to fissility. Evidently, such nature of changes in a velocity with pressure depends upon a type of deformation and subsequent disintegration of the stratified-anisotropic media. Transversal deformation progresses faster to compare with axial deformation (velocity decrease and negative increment sign); pores and microfissures, oriented along layers, are filled simultaneously. Then, intensive growth of transversal deformation comes to its end (knee point) and increase in a compressional wave velocity starts with pressure increase (a sign of relative velocity increment varies to a positive one).

Lab environment demonstrates significant decrease in anisotropic coefficients of the laminated limestones and micaceous-quartz shales depending upon pressure increase (Fig. 4); moreover, the majority of the changes are observed in terms of pressures being 20-30% of critical ones. Then, the changes slow down. If pressure is ~50% of a critical one anisotropy coefficient of the laminated limestones decreases averagely by 40-50 down to 7-12%; in terms of micaceous-quartz shales the decrease is 80-100 down to 30-40% respectively.

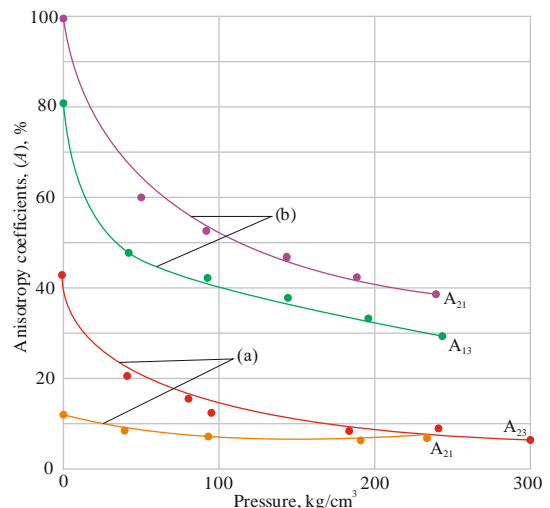


Figure 4. Changes in anisotropy coefficient with pressure: a is for the laminated limestones; and b is for micaceous-quartz shales

As it has been mentioned, the laminated limestones experience their disintegration faster if loading is along fissility ($\sigma_{comp} = 610 \text{ kg/cm}^2$). The disintegration takes place due to breakage of intergranular contacts. In this context, the veloci-

ty, measured transversely to fissility decreases depending upon rock decompression; in turn, velocity anisotropy increases. If the loading is transversely to fissility then rocks experience their disintegration in terms of higher loads ($\sigma_{comp}^{\perp} = 800 \text{ kg/cm}^2$). Intergranular contacts become more compact; velocity of compressional waves transversely to fissility increases; and velocity anisotropy decreases. Namely, changes in values of anisotropy coefficients of elastic wave velocities may be associated virtually with availability of stresses directed horizontally or vertically to layers.

Consequently, anisotropy of compressional wave velocities depends upon the applied pressure varying according to it. In other words, anisotropy of a compressional wave velocity depends upon stress state of rocks. However, the correlation is understudied.

3.3. Study of correlation between rock characteristics and conditions

Studies prove the pronounced velocity increase along with rock strength increase. For instance, rocks of marble and Chat-Bazar limestone type, being notable for their maximum homogeneity and isotropism, demonstrate rather high velocity-strength correlation ($r = 0.86$). In the context of the rocks, strength anisotropy coefficient, identified on $K = \sigma^{\perp}/\sigma^{\parallel}$ values, is close to 1. Rocks of Uluu-Too deposit (effusives, listvenites, shales, and serpentinites) are characterized by significant homogeneity and anisotropy; as a result, in this case correlation coefficient is low ($r = 0.64$). As for the anisotropic rocks, values of strength characteristics depend upon load application lines as well as upon directions of elastic symmetry axes.

Anisotropic micaceous-quartz shales, the silicified jasperoids, the laminated limestones, and shales experienced the unconfined compressive strength test in terms of different load orientations relative to layers (Fig. 5).

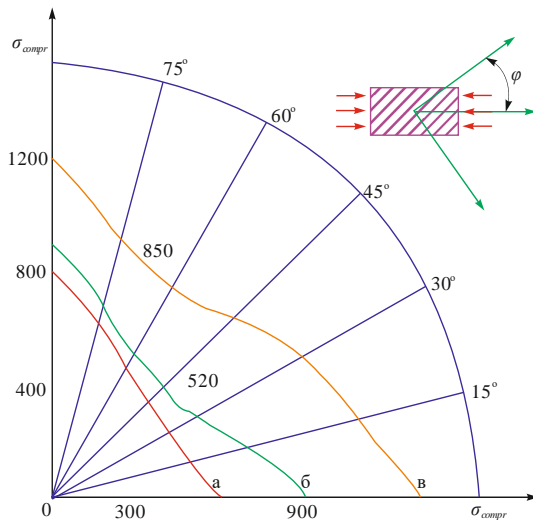


Figure 5. Dependence of rock strength in terms of uniaxial compression depending upon incidence angles of the layers: a is the laminated limestone; b is jasperoid; and c is micaceous-quartz shale

As it is understood from Figure 5, σ_{comp} values, obtained for micaceous-quartz shales along fissility and transversely to it, are almost similar. Their minimal resistance has been demonstrated in the line where 45° angle with layer direction is available. In this context, $\sigma_{comp}^{45^\circ} = 525 \text{ kg/cm}^2$ being 60%

of $\sigma_{comp}^{90^\circ}$. As for the jasperoids, ultimate compression strength, measured at 60° with $\sigma_{comp}^{65^\circ} = 850 \text{ kg/cm}^2$ layer direction, is a determinative factor. It is ~70% of $\sigma_{comp}^{90^\circ}$. In terms of carbonaceous shales and the laminated limestones, minimal σ_{comp} value corresponds to the case when layer direction coincides with a loading line.

In the majority of cases, strength anisotropy of rock may be reduced to availability of the certain systems of loosening surfaces in it when rock shear force and tension strength deteriorate to compare with the basic mass of the rock.

In the context of the unconfined compressive strength test along layers on the condition that friction is not available and elastic behavior of rock matrix as well as a binding material is almost similar, a surface over which disintegration takes place coincides with direction of interlayers failed by microfissures. Disintegration has a form of separation.

Many authors consider strength anisotropy separately from analysis of elastic characteristic anisotropy; however, velocity-strength correlations for isotropic rocks are known.

Increase in elastic anisotropy coefficient is followed by the increase in strength anisotropy; in turn, decrease in elastic anisotropy value results in the increased uniaxial compression strength (Table 1).

Nevertheless, as it appears from the experimental data (Fig. 5) the process is not constant. As for the micaceous-quartz shales, characterized by orthotropic elastic symmetry, anisotropy of strength properties along the key anisotropic axes is less than 10%. In other words, anisotropy of elastic wave velocities as it is evaluated in this case, may characterize anisotropy of rock strength with the help of transverse-isotropic elastic symmetry only. Higher velocities of compressional waves correspond to the toughest rocks. Moreover, in terms of rocks with high homogeneity coefficient, spread of values of an average one is $\Delta p = \pm 0.024 \text{ g/cm}^2$.

In the context of Uluu-Too deposit rocks, characterized by structural nonhomogeneity and fissility, absolute error of rock density identification on the value of compressional wave velocity is significant. That is to say, qualitative evaluation of rock density according to velocities of elastic waves is possible for rocks with high homogeneity coefficient. Homogeneity coefficient and anisotropy coefficient were determined ultrasonically on the value of compressional wave velocity:

$$K_0 = \frac{\overline{V_P} - 3\sqrt{\frac{\sum_{i=1}^n (V_P - V_{Pi})^2}{n}}}{\overline{V_P}}, \quad (54)$$

where:

V_P – average velocity of a compressional wave along one direction, m/sec;

V_{Pi} – one of velocity values, m/sec;

n – measurement number.

In the context of anisotropic waves, characterized by distinctly varying velocity values in terms of different directions, it seems to be dilemmatic to evaluate their density.

Elastic wave velocities (V_P , V_S , V_R) were measured using methods of through scanning of in-line profiling, and transversal one. In case of anisotropic rocks which anisotropy coefficient is more than 8% profiling should be performed involving three orthogonal profiles with the development of phase hodographs for each line.

Table 1. Correlation between elastic anisotropy and strength characteristics

Rock	Velocity of elastic waves, m/sec		Anisotropy coefficient of velocity of elastic waves, %	Ultimate compression strength, kg/cm ²		Coefficient of strength anisotropy, % $K = \frac{\sigma_{max} \cdot \sigma_{min}}{\sigma_{min}}$
	V_{P1}	$V_{P\perp}$		σ_{max}	σ_{min}	
	Basalt	4610		4410	4.5	
Marmorized limestones	5460	5100	6.8	865	830	4.1
Chloritic shale	7120	6400	11.3	3140	2400	30.8
Jasperoids	4760	4050	17.0	1290	850	51.9
Laminated limestones	4740	3280	44.6	805	610	32.0
Carbonaceous shales	5105	2715	87.5	1400	830	68.6
Micaceous-quartz shales	5100	2550	100.0	880	525	68.1

Anisotropy coefficient along any profile is determined using the formula:

$$A = \frac{V_{Px} - V_{Pz}}{V_{Pz}} \cdot 100\%, \tag{55}$$

where:

- V_{Px} – compressional wave velocity towards x axis, m/sec;
- V_{Pz} – compressional wave velocity towards z axis;
- n – measurement number.

In case of anisotropic rocks, analysis of elastic, strength, and deformational characteristics should start from determination of occurrence orientation and analytical model. For the purpose, 30×30×30 cm rock blocks were applied for through scanning to identify directions of maximum and minimum values of compressional wave velocities.

Three orthogonal planes are selected at one of monolith angle for more accurate determination of spatial orientation of the samples. Each plane is divided into several profiles, concurring and shifted relative to each other to 11, 22, 5 or 45° (Fig. 6). The total of diagrams of velocity distribution within the three orthogonal planes is used to single out lines of maximum, minimum, and intermediate values of velocities of compressional waves.

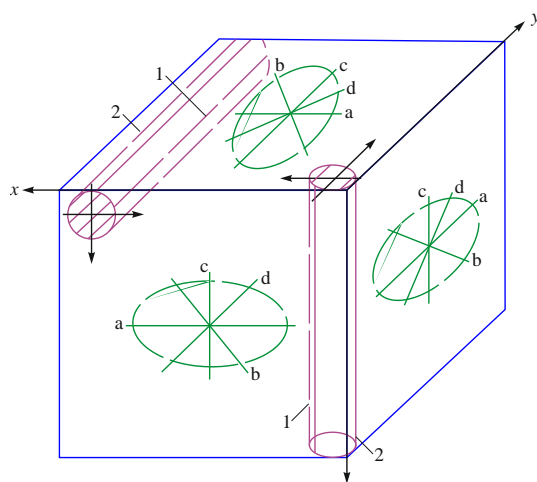


Figure 6. Scanning scheme for blocks of anisotropic rocks

Three orthogonal planes are selected at one of monolith angle for more accurate determination of spatial orientation of the samples. Each plane is divided into several profiles, concurring and shifted relative to each other to 11, 22, 5 or 45° (Fig. 6). The total of diagrams of velocity distribution within the three orthogonal planes is used to single out lines of maximum, minimum, and intermediate values of velocities of compressional waves.

Results of the analysis, carried out using the laminated limestones, have helped identify that the coefficient of velocity anisotropy, defined on the ratios of axial velocities, measured along fissility and transversely to it, is 1.43. Thus, acoustic characteristics and elastic characteristics differ greatly in terms of orthogonal directions. Values of compressional waves, measured within stratification planes with the help of radial profiles, oriented to each other at different angles, do not depend upon the direction of propagation of the waves. They are equal in terms of reasonable errors. Average velocity of a compressional wave along stratification is $\overline{V_p} = 4550 \pm 70$ m/sec; it is $\overline{V_s^{\parallel}} = 2520 \pm 90$ m/sec for transversal wave; and $\mu^{\parallel} = 0.27$. Determination of velocities of elastic waves within planes, making a certain angle with the stratification plane, has shown that along with the angle increase, acoustic parameters of the rock decrease becoming a minimum transversely to the stratification (Table 2).

Similar measurements were performed for other rocks under study. It has been obtained that in the context of shales and laminated limestones from Khaidarkan deposit, analytical anisotropy model with transverse-isotropic elastic symmetry is typical. In this case, stratification plane is isotropic plane. To calculate elastic characteristics of such a medium, it is required to know V_p and V_s velocities, measured within two orthogonal planes.

Moisture exercises a significant influence on the velocities of compressional waves, and anisotropy coefficient of compressional waves of the laminated limestones. To identify the influence, the samples were moistened up to complete saturation. While saturating, compressional wave velocities were measured. After complete water saturation, velocity anisotropy coefficient decreased from 1.45 down to 1.20. Apparently, the fact can be explained by intensive increase in a compressional wave velocity transversely to a layer to compare with changes in a compressional wave velocity along the layer. The abovementioned depends upon textural changes during humidification.

In contrast to shales and laminated limestones from Khaidarkan deposit, micaceous-quartz shales and amphibolites from Tereksay deposit are characterized by orthotropic anisotropy scheme. Velocities of compressional ways, measured to the dip, along the strike, and transversely to stratification, differ greatly (Table 3).

Anisotropy degree of elastic oscillation velocities was evaluated using (54)-(55) formulas and methods of the oriented profiling. Values of anisotropy coefficients, calculated on the velocities of P - and S -waves, do not coincide. Generally, values of anisotropy coefficients for transversal waves are lower than those for compressional waves. However, they have not any single-valued correlation.

Table 2. Velocimetry of compressional and transversal waves measured at different angles to the stratification plane

Laboratory number of a sample	Velocity of a compressional wave V_P , m/sec				Velocity of a transversal wave V_S , m/sec				Poisson's ratio		Anisotropy coefficient $A_K = \frac{V_{P\parallel}}{V_{P\perp}}$
	0°	30°	60°	90°	0°	30°	60°	90°	μ_{\parallel}	μ_{\perp}	
1	4570	4050	3400	3200	2420	2380	2300	1980	0.30	0.19	1.41
2	4600	4070	3280	3180	2530	2290	2060	1880	0.28	0.22	1.45
3	4510	3800	3170	3030	2245	2300	2170	1910	0.31	0.16	1.48
4	4560	3680	3360	3060	2640	2470	3200	1900	0.23	0.17	1.19
5	4500	4140	3200	3020	2700	2540	2100	1720	0.21	0.26	1.49
6	4660	4050	3570	3200	2420	2340	2210	1950	0.27	0.20	1.45
7	4350	3380	3160	3040	2540	2280	2080	1690	0.25	0.27	1.43
8	4700	3870	3380	3290	2540	2300	1700	1560	0.29	0.33	1.43

Table 3. Average values of velocities of elastic waves and anisotropy coefficients of compressional waves for the rocks under study

Rock	Compressional wave velocity, m/sec			Transversal wave velocity, m/sec			Anisotropy coefficient of velocities of compressional waves, %			Anisotropy coefficient of velocities of transversal waves, %		
	V_{Px}	V_{Py}	V_{Pz}	V_{Sx}	V_{Sy}	V_{Sz}	A^p_{yx}	A^p_{yz}	A^p_{xz}	A^s_{yx}	A^s_{yz}	A^s_{xz}
Micaceous-quartz shales	5130	4370	2540	2880	2500	1540	17.5	102.4	72.2	15.6	88.0	63.3
Amphibolites	6000	5630	5080	2970	3010	2650	6.6	18.3	10.9	5.5	12.4	13.5
Laminated limestones	4610	–	3190	2460	–	1930	–	45.0	–	–	23.4	–
Silicified jasperoids	4770	–	3930	2400	–	2180	–	21.0	–	–	11.1	–
Siliceous shales	5060	5000	4450	2940	2800	1980	1.2	13.7	12.3	5.0	48.4	41.4
Marmorized limestones	5450	5380	5100	3160	3280	3190	1.3	6.8	5.4	3.6	1.0	2.8

Elastic characteristics have been defined for the analyzed rocks taking into consideration analytical anisotropy scheme and using formulas (30), (31), (36), and (50)-(52) to calculate elastic characteristics of anisotropic rocks with orthotropic, and transverse-isotropic symmetry (Table 4).

Table 4. Elastic characteristics of anisotropic and isotropic rocks under study

Rock	Elastic characteristics		
	$E_x \cdot 10^5$, kg/cm ²	$E_y \cdot 10^5$, kg/cm ²	$E_z \cdot 10^5$, kg/cm ²
Micaceous-quartz shales	5.77	4.99	1.41
Amphibolites	7.48	6.61	5.35
Laminated limestones	4.80	–	2.26
Silicified jasperoids	4.35	–	3.13
Shales	6.71	–	5.22
Siliceous shales	5.80	6.19	4.48
Marmorized limestones	7.00	6.76	6.2
Jasperoids	5.58	5.56	5.60

As it is understood from Tables 3 and 4, the rocks are characterized by significant anisotropy of velocities of elastic waves varying broadly (i.e. 5-10 to 80-100%). Elastic characteristics, measured in terms of different direction relative to symmetry axes, differ significantly too.

Elasticity moduli, determined in the line of stratification E_1 , G_1 , μ_1 , are larger than those, determined transversely to stratification E_{\perp} , G_{\perp} , μ_{\perp} ; so, $E_1 > E_{\perp}$, $G_1 > G_{\perp}$, $\mu_1 > \mu_{\perp}$ ratios take place. While comparing Tables 3 and 4, one can deduce easily that relative the abovementioned occurrence components, n^2 times variation of compressional wave velocity corresponds to n^2 times variation of elasticity modulus and shear modulus in terms of corresponding directions. In other words, the greater anisotropy degree is, the more significant is difference in the parameters determined in terms of the directions.

The research of anisotropic samples has demonstrated that rock strength characteristics are functions of the oriented

rock microstructure which depend upon a line of load application relative to fissility. In accordance with structural and textural features, minimum and maximum strength values not always coincide with layer direction. In terms of micaceous-quartz shales, minimum strength value is when layers are located at 45° towards load action; the angle is 60° for the silicified jasperoids. In terms of carbonaceous shales and limestones, minimum strength value corresponds to a case when loading line coincides with layer direction; maximum value is when the process takes place transversely to layers. Reason of such differences is in the mechanism of anisotropic sample disintegration.

In the context of all mechanical experiments, large strength indices always corresponded to directions of large velocity values of elastic waves. Increase in a velocity anisotropy coefficient, i.e. decrease in elastic anisotropy value results in the increased uniaxial compression strength.

Determination of acoustic V_P , V_S , A_{ik} and elastic E , G , μ rock indices when analytical scheme of rock anisotropy was taken into consideration has helped identify that the rocks under study are characterized by their own significant anisotropy. Analysis of the results supports the idea that the larger degree of velocity anisotropy is, the greater elastic parameters, defined for different orientations relative to occurrence components, vary.

Elasticity moduli, calculated on the elasticity theory formulas for isotropic body, differ from each other by 50-60%. If they are calculated according to formulas for anisotropic rocks, the difference reduced down to 20-25%.

Laboratory unconfined compressive strength tests with simultaneous scanning have made it possible to define the following. Pressure exercises a significant influence on the velocity of compressional waves. If load increases 0 to 50% of destructive one then $V_P^{\perp}(p)$ velocity for the rocks under study increases by 25-35%; the increase is 7-15% for $V_P^{\parallel}(p)$. Nonlinear correlation is between compressional wave velocity and compression stress.

A curve of velocity of a compressional wave change along layers is above a curve of a velocity change transversely to layers. Hence, the rocks are characterized by anisotropy of velocities of elastic oscillations and under pressure.

Degree of $V(p)$ variation in terms of loads, oriented differently to fissility, is not identical, and depends upon textural features of a medium; anisotropy decrease is observed in terms of loading being transverse to fissility. The anisotropy increases while loading along fissility.

Under laboratory conditions, anisotropy coefficients of velocities of compressional wave demonstrate significant decrease along with pressure increase. Considerable part of the changes falls on pressure being 20-30% of failure one.

The research helps determine dependences of elastic characteristics upon pressure and depth; moreover, they explain a pattern of absolute and relative stress distribution within rock mass in the neighbourhood of mine workings. However, to compare with the specific laboratory experiments, in-situ rocks experience effect of numerous factors as well as rather complex stress field.

That is why the only way to obtain reliable information concerning stress distribution within the specific area of the Earth's crust is to perform immediate measurements of stress state of rocks in mine workings; experiments remain the basic research method.

4. Conclusions

Dynamic elastic characteristics of anisotropic rock with orthotropic elastic symmetry should be determined through values of compressional and transversal wave velocity along the basic directions of elastic symmetry axes, and values of velocities of transversal waves at 45° angle to the key directions.

The obtained quantitative dependences make it possible to calculate elastic characteristics of anisotropic rocks in terms of velocities of compressional and transversal waves, measured along the key axes of elastic symmetry, and velocities of transversal waves at 45° angle to the key directions.

To verify the derived quantitative dependences, it is necessary to define a type of analytical scheme of anisotropy the rock belongs to: media with orthotropic or transverse-isotropic elastic symmetry. The abovementioned is connected with determination of values as well as the key anisotropy directions of the rocks under study.

Laboratory unconfined compressive strength tests with simultaneous scanning have helped identify the following:

- pressure exercises a significant influence on the velocity of compressional waves. In terms of 0 to 50% of a failure load increase, $V_{p^{\perp}}(p)$ velocity enhancement is 25-35%; the increase is 7-15% for $V_{p^{\parallel}}(p)$ velocity. Nonlinear correlation is between compressional wave velocity and compression stress;
- curve of velocity of a compressional wave change along layers is above a curve of a velocity change transversely to layers. Hence, the rocks are characterized by anisotropy of elastic oscillation velocities and under pressure;
- $V(p)$ change degree in terms of loading, oriented differently to fissility, is not identical and depends upon textural features of a medium; anisotropy decrease is observed in terms of loading being transverse to fissility. The anisotropy increases while loading along fissility;
- lab environment demonstrates significant decrease in anisotropy coefficients of the laminated limestones and

micaceous-quartz shales depending upon pressure increase; moreover, the majority of the changes are observed in terms of pressures being 20-30% of critical ones.

Consequently, the research helps determine dependences of elastic characteristics upon pressure and depth; moreover, they explain a pattern of absolute and relative stress distribution within rock mass in the neighbourhood of mine workings. $A = 1.45$, obtained for the laminated limestones, and $A = 1.200$, obtained for carbonaceous shale are the essential and necessary conditions to consider stress state.

However, to compare with the specific laboratory experiments, in-situ rocks experience effect of numerous factors as well as rather complex stress field.

Thus, obtaining of reliable information concerning stress distribution within the specific area of the Earth's crust involves further research to develop criteria of evaluation and stability control of rock mass around a mine working using acoustic module on the basis of quantitative consideration of anisotropy A influence through velocities of elastic waves V_p and V_s .

Acknowledgements

The authors express gratitude to Shergazy Asambayevich Mambetov, Professor of Kyrgyz Russian Slavic University for academic advising, valuable help, and instructions; and to Professor Kamchybek Chonmurunovich Kozhogulov for support in the research pursuance in the laboratories of Institute of Rock Mechanics and the Earth's Interior Development of the National Academy of Sciences of Kyrgyz Republic. The research is not supported by a project or financing.

References

- [1] Majkherchik, T., Gajko, G.I., & Malkowski, P. (2002). Deformation process around a heading investigation when front of longwall face advancing. *Ugol*, (11), 27-29
- [2] Abdiev, A.R. (2002). Evaluation of the stressed-strained state of rock massif for brown coal deposit in Kara-Keche. *Gornyi Zhurnal*, (10), 70-72.
- [3] Abdiev, A.R., Mambetova, R.S., & Mambetov, S.A. (2017). Geomechanical assessment of Tyan-Shan's mountains structures for efficient mining and mine construction. *Gornyi Zhurnal*, (4), 23-28. <https://doi.org/10.17580/gzh.2017.04.04>
- [4] Shashenko, O., Shapoval, V., Khalymendyk, O., Andrieiev, V., Arbuzov, M., Hubar, O., & Markul, R. (2019). Features of the nonlinear calculation of the stress-strain state of the "Rock massif-excavation support" system taking into account destruction. *Transport Means – Proceedings of the International Conference*, 1356-1363.
- [5] Arshamov, Y., Seitmuratova, E., & Baratov, R. (2015). Perspectives of porphyry copper mineralizations in Zhongar-Balkhash fold system. *International Multidisciplinary Scientific GeoConference Surveying Geology and Mining Ecology Management*, 345-350.
- [6] Baibatsha, A., Arshamov, Y., Bekbotayeva, A., & Baratov, R. (2017). Geology of the main industrial types of copper ore deposits in Kazakhstan. *International Multidisciplinary Scientific GeoConference, Science and Technologies in Geology, Exploration and Mining*, 17(11), 231-238. <https://doi.org/10.5593/sgem2017/11/s01.029>
- [7] Mambetov, S.A., Mambetov, A.S., & Abdiev, A.R. (2002). Zonal and step-by-step evaluation of the stressed-strained state of Tyan'-Shan' rock massif. *Gornyi Zhurnal*, (10), 57-62.
- [8] Bondarenko, V., Symanovych, G., & Koval, O. (2012). The mechanism of over-coal thin-layered massif deformation of weak rocks in a longwall. *Geomechanical Processes During Underground Mining*, 41-44. <https://doi.org/10.1201/b13157-8>
- [9] Abdykapparov, C.M., & Abdiev, A.R. (2002). State and prospects of the development the brown coal deposit in Kara-Keche. *Gornyi Zhurnal*, (10), 16-19.
- [10] Sotskov, V., & Saleev, I. (2013). Investigation of the rock massif stress strain state in conditions of the drainage drift overworking. *Annual Sci-*

- entific-Technical Collection – *Mining of Mineral Deposits*, 197-201. <https://doi.org/10.1201/b16354-35>
- [11] Sharapatov, A., Shayahmet, M., & Arshamov, Y.K. (2016). About modern technology field geophysical research areas sulfide mineralization in western Kazakhstan. *News of the National Academy of Sciences of the Republic of Kazakhstan, Series of Geology and Technical Sciences*, 1(415), 102-107.
- [12] Sejtмуратова, Е.Ж., Аршамов, Ж.К., Баратов, Р.Т., Даутбеков, Д.О. (2016). Geological and metallogenic features of volcano-plutonic belt Kazakhstan. *News of the National Academy of Sciences of the Republic of Kazakhstan, Series of Geology and Technical Sciences*, 3(416), 60-86.
- [13] Razin, A.V., & Sobisevich, A.L. (2012). *Geoakustika sloistykh sred.* Moskva, Rossiya: IFZ RAN.
- [14] Kapitonov, A.M., & Vasil'yev, V.G. (2011). *Fizicheskie svoystva gornykh porod zapadnoy chasti Sibirskoy platformy.* Krasnoyarsk, Rossiya: SibFU.
- [15] Abdiev, A.R., Mambetova, R.Sh., & Abdiev, A.A. (2020). Izuchenie deformatsiy porodnykh massivov vysokogornykh mestorozhdeniy, prognos i kontrol' ikh geomekhanicheskogo sostoyaniya. *Tendentsii Razvitiya Nauki i Obrazovaniya*, (60), 51-57.
- [16] Voznesenskiy, A.S., Kutkin, Ya.O., & Krasilov, M.N. (2015). Vzaimosvyaz' akusticheskoy dobrotnosti s prochnostnyimi svoystvami izvestyakov. *FTPRPI*, (1), 30-39.
- [17] Mambetov, Sh.A., Mambetov, A.Sh. (2018). *Geoakusticheskie metody izucheniya porodnogo massiva.* Bishkek, Kyrgyzstan: KRSU.
- [18] Gorbatevich, F.F. (2019). K probleme otsenki uprugoy anizotropii gornykh porod kvaziortotropnoy simmetrii. *Fizika Zemli*, 130-139.
- [19] Abdiev, A.R., Mambetova, R.Sh., & Abdiev, A.A. (2020). Sovershenstvovanie tekhnologii i organizatsii geologicheskogo izucheniya ekspluatiruemyykh slozhnostrukturnyykh mestorozhdeniy. *Tendentsii Razvitiya Nauki i Obrazovaniya*, (60), 57-64.
- [20] Mambetov, Sh.A., Abdiev, A.R., & Mambetov, A.Sh. (2003). *Zonal'naya i poetapnaya otsenka porodnogo massiva Tyan'-Shanya.* Bishkek, Kyrgyzstan: KRSU.
- [21] Mambetov, Sh.A., Abdiev, A.R., & Mambetov, A.Sh. (2012). Geomekhanicheskoe obespechenie gornykh rabot v usloviyakh vysokogor'ya. *Inzhener*, 3(4), 29-36.
- [22] Abdiev, A.R., Mambetova, R.Sh., Abdiev, A.A., & Abdiev, Sh.A. (2020). Aktual'nye voprosy kontrolya sostoyaniya porodnogo massiva vokrug gornoy vyrabotki. *Nedropol'zovanie XXI Veka*, (2), 82-91.
- [23] Abdiev, A.R. (2020). Razrabotka sposobov prognozirovaniya geomekhanicheskikh protsessov v porodnykh massivakh. *Problemy Nedropol'zovaniya*, (1), 49-55.
- [24] Mambetov, Sh.A., Abdiev, A.R., & Izabaev, K.D. (2015). Strukturno-mekhanicheskie osobennosti porodnogo massiva Tyan'-Shanya i voprosy prognozirovaniya sostoyaniya porodnogo massiva mestorozhdeniy. *Vestnik KRSU*, 15(9), 191-197.
- [25] Abdiev, A.R., Izabaev, K.D., & Mambetov, Sh.A. (2016). Priroda i zakonmernosti proyavleniya negativnykh geomekhanicheskikh faktorov pri vedenii gornykh rabot na vysokogornykh mestorozhdeniyakh. *Simvol Nauki*, 12(3), 263-266.
- [26] Mambetov, Sh.A., & Abdiev, A.R. (2019). *Geomekhanicheskoe sostoyanie porodnogo massiva Tyan'-Shanya.* Bishkek, Kyrgyzstan: KRSU.
- [27] Abdiev, A.R., Mambetova, R.Sh., Abdiev, A.A., & Abdiev, Sh.A. (2020). Aktual'nye voprosy kontrolya sostoyaniya porodnogo massiva vokrug gornoy vyrabotki. *Nedropol'zovanie XXI Veka*, 2(85), 82-90.
- [28] Abdiev, A.R. (2020). Prognozirovanie i otsenka geomekhanicheskikh protsessov v porodnykh massivakh mestorozhdeniy. *Problemy Nedropol'zovaniya*, (1), 56-64.
- [29] Mikhlin, Y.V., & Zhupiev, A.L. (1997). An application of the ince algebraization to the stability of non-linear normal vibration modes. *International Journal of Non-Linear Mechanics*, 32(2), 393-409. [https://doi.org/10.1016/s0020-7462\(96\)00047-9](https://doi.org/10.1016/s0020-7462(96)00047-9)
- [30] Shashenko, A., Gapieiev, S., & Solodyankin, A. (2009). Numerical simulation of the elastic-plastic state of rock mass around horizontal workings. *Archives of Mining Sciences*, 54(2), 341-348.
- [31] Mambetov, Sh.A., & Abdiev, A.R. (2017). Geomekhanicheskoe sostoyanie porodnykh massivov vysokogornykh mestorozhdeniy. *Vestnik KRSU*, 17(5), 140-143.
- [32] Abdibaitov, Sh.A., Isaev, B.A., & Abdiev, A.R. (2017). Vliyanie fiziko-mekhanicheskikh svoystv i strukturnyykh narusheniy porod na protsess obrazovaniya provalov zemnoy poverkhnosti. *Vestnik KRSU*, 17(8), 140-143.
- [33] Sudakov, A., Dreus, A., Sudakova, D., & Khaminich, O. (2018). The study of melting process of the new plugging material at thermomechanical isolation technology of permeable horizons of mine opening. *E3S Web of Conferences*, (60), 00027. <https://doi.org/10.1051/e3sconf/20186000027>
- [34] Seitmuratova, E., Arshamov, Y., Bekbotayeva, A., Baratov, R., & Dautbekov, D. (2016). Priority metallogenic aspects of late paleozoic volcanic-plutonic belts of Zhongar-Balkhash fold system. *International Multidisciplinary Scientific GeoConference Surveying Geology and Mining Ecology Management*, (1), 511-518. <https://doi.org/10.5593/sgem2016/b11/s01.064>
- [35] Galiyev, D. (2020). Modelling hydraulic mixture movement along the extraction chamber bottom in case of hydraulic washout of the puffstone. *E3S Web of Conference*. Preprint.
- [36] Sudakov, A., Chudyk, I., Sudakova, D., & Dziubyk, L. (2019). Innovative technology for insulating the borehole absorbing horizons with thermoplastic materials. *E3S Web of Conferences*, (123), 01033. <https://doi.org/10.1051/e3sconf/201912301033>

Дослідження взаємозв'язку властивостей та стану порід

А. Абдієв, Р. Мамбетова, А. Абдієв, Ш. Абдієв

Мета. Встановлення залежностей швидкостей пружних хвиль в ізотропних та анізотропних породах з ортотропною і трансверсально-ізотропною симетрією, від тиску та глибини, для розробки критеріїв оцінки й контролю властивостей і стану породного масиву поблизу гірничих виробок.

Методика. Розглядається суцільне анізотропне середовище. Перша група умов на межі являється умовами безперервності напружень, що діють нормально до межі при переході з шару 1 в шар 2. Друга група граничних умов полягає в тому, що зміщення при переході через межу вимірюються також безперервно. Ці умови є необхідними для виконання рівняння динамічної рівноваги пружного середовища Новьє-Стокса. Експериментальні дослідження виконувалися геоакустичним методом за акустичним параметром швидкості поздовжньої хвилі.

Результати. Встановлено, що величини швидкостей пружних хвиль, анізотропія швидкостей поздовжніх хвиль, пружні характеристики закономірно відображають особливості будови і залежать від тиску. Виявлено, що залежно від напруженого стану відзначаються випадки зникнення чи появи анізотропії, або зміни знаку на зворотний. Отримано кількісні залежності з визначення пружних характеристик (E , μ , G) анізотропного масиву з ортотропною, трансверсально-ізотропною симетрією через швидкості пружних хвиль для правильного обліку анізотропії властивостей масиву при оцінці його напруженого стану. Результати досліджень дозволять оцінити характер розподілу напружень, виявити зони концентрації напружень і зони порушення порід поблизу гірничої виробки за акустичним параметром швидкості поздовжньої хвилі розробленого авторами методом геоакустичного контролю.

Наукова новизна. Згідно нових отриманих залежностей, науково визначені значення пружних характеристик гірських порід (E , μ , G) та акустичні параметри швидкості поздовжньої хвилі, що є цінними для проектування й планування розвитку гірничих робіт.

Практична значимість. Отримані результати досліджень, з достатньою для практичного застосування точністю, можуть використовуватися для визначення числових значень пружних характеристик (E , μ , G), дають можливість застосування методу геоакустичного контролю властивостей і стану породного масиву поблизу гірничих виробок і залучати до відпрацювання родовища зі складними структурно-механічними особливостями.

Ключові слова: ізотропні та анізотропні породи, напруження гірських порід, пружні характеристики, акустичний параметр, швидкість поздовжньої хвилі, геоакустичний контроль

Исследование взаимосвязи свойств и состояния пород

А. Абдиев, Р. Мамбетова, А. Абдиев, Ш. Абдиев

Цель. Установление зависимостей скоростей упругих волн в изотропных и анизотропных породах с ортотропной и трансверсально-изотропной симметрией, от давления и глубины, для разработки критериев оценки и контроля свойств и состояния породного массива вблизи горных выработок.

Методика. Рассматривается сплошная анизотропная среда. Первая группа условий на границе представляется условиями непрерывности напряжений, действующих нормально к границе при переходе из слоя 1 в слой 2. Вторая группа граничных условий состоит в том, что смещение при переходе через границу измеряются также непрерывно. Эти условия являются необходимыми для выполнения уравнения динамического равновесия абсолютно упругой среды Новье-Стокса. Экспериментальные исследования выполнялись геоакустическим методом по акустическому параметру скорости продольной волны.

Результаты. Установлено, что величины скоростей упругих волн, анизотропия скоростей продольных волн, упругие характеристики закономерно отражают особенности строения и зависят от давления. Выявлено, что в зависимости от напряженного состояния отмечаются случаи исчезновения или появления анизотропии, или перемены знака на обратный. Получены количественные зависимости по определению упругих характеристик (E , μ , G) анизотропного массива с ортотропной, трансверсально-изотропной симметрией через скорости упругих волн для правильного учета анизотропии свойств массива при оценке его напряженного состояния. Результаты исследований позволят оценить характер распределения напряжений, выявить зоны концентрации напряжений и зоны нарушенных пород вблизи горной выработки по акустическому параметру скорости продольной волны разработанным авторами методом геоакустического контроля.

Научная новизна. Согласно новым полученным зависимостям научно определены значения упругих характеристик горных пород (E , μ , G), и акустические параметры скорости продольной волны, ценные для проектирования и планирования развития горных работ.

Практическая значимость. Полученные результаты исследований, с достаточной для практического применения точностью, могут использоваться для определения числовых значений упругих характеристик (E , μ , G), дают возможность применения метода геоакустического контроля свойств и состояния породного массива вблизи горных выработок и привлекать к отработке месторождений со сложными структурно-механическими особенностями.

Ключевые слова: *изотропные и анизотропные породы, напряжение горных пород, упругие характеристики, акустический параметр, скорость продольной волны, геоакустический контроль*

Article info

Received: 26 March 2020

Accepted: 3 August 2020

Available online: 4 September 2020